Rohner et al., http://www.jcb.org/cgi/content/full/jcb.201207024/DC1

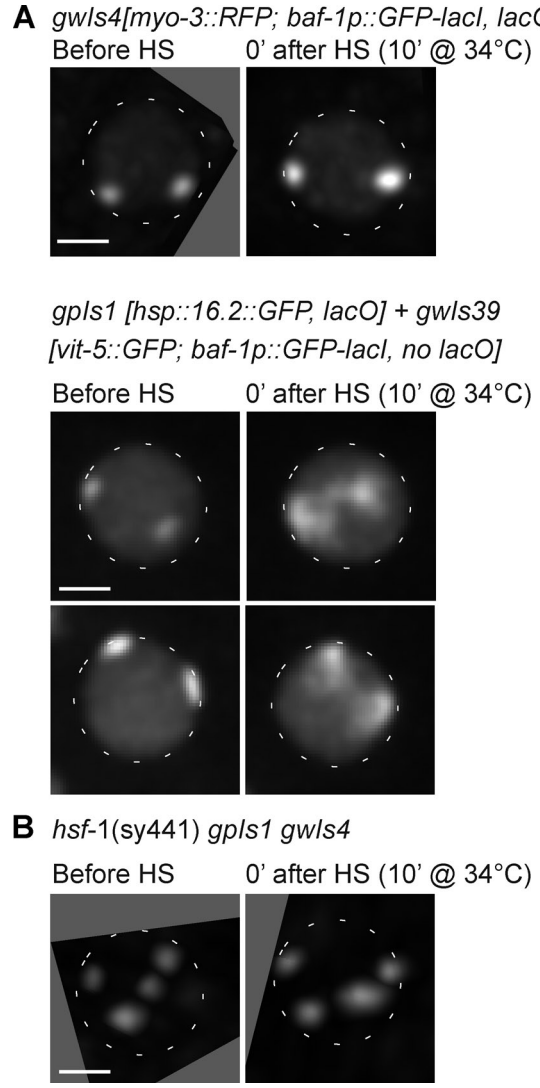

Figure S1. **Controls for the induced integrated array of *hsp-16.2* promoter.** (A) HS does not induce decondensation of a large array bearing *baf-1* promoter–driven GFP-lacI in embryos. Nuclei from an embryo of a strain carrying only the GFP-lacI–expressing array *gwIs4* are shown before and after HS. No change in array shape is observed upon HS. (B) *hsf-1(sy441)* impairs decondensation of HS-activated arrays. In a strain carrying both a GFP-lacI–expressing array (*gwIs4*) and an HS-activated array (*gpIs1*), no difference in size can be observed before and after HS. Each nucleus is encircled by a broken line. Bars, 2 µm.

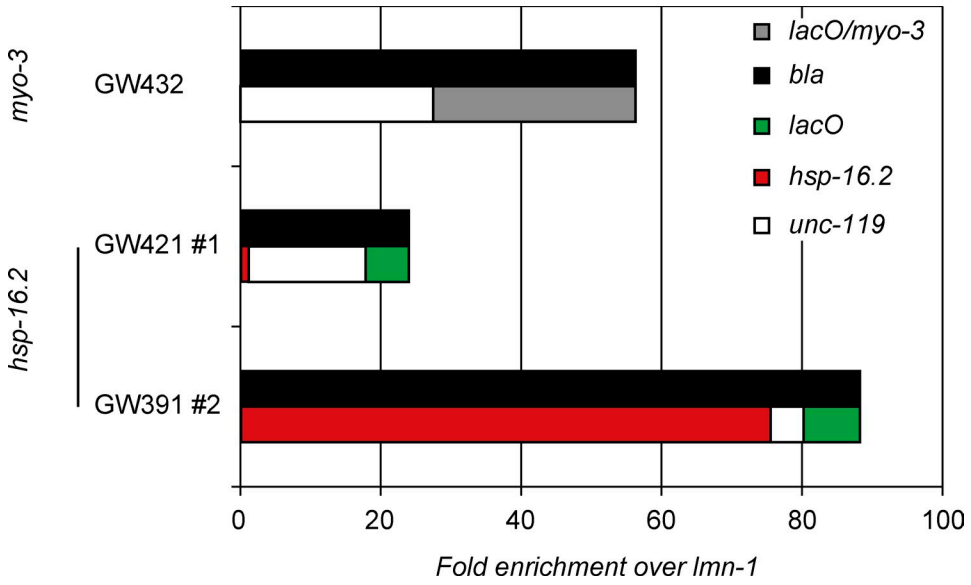

Figure S2. **Quantification by real-time PCR of the number of plasmids present in the small arrays carrying *hsp-16.2::mCherry*.** Copy numbers of plasmids found in integrated transgenes shown in Fig. 2 D were determined for *unc-119*, *hsp-16.2*, and the *bla* sequences (present in all plasmids). Normalization of PCR efficiency for *unc-119* and *hsp-16.2* was achieved using WT worms. The *lacO* copy number was calculated by subtracting the *unc-119* and *hsp-16.2* plasmid number from the total *bla* copy number.

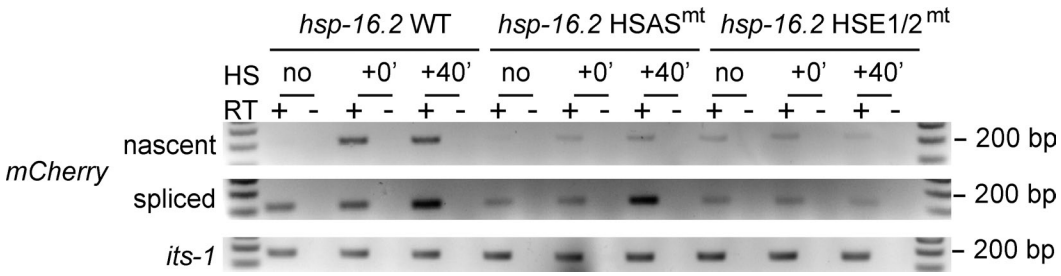

Figure S3. **PCR amplification detects *mCherry* mRNA in a reverse transcription–dependent manner.** Nascent and spliced RNAs were detected by real-time PCR of RNA driven from the indicated mutant *hsp-16.2* promoters in the MosSCI integration. The levels are extremely low when normalized to *its-1* (Fig. 5). Detection of transcripts is nonetheless possible after 30 cycles of normal PCR using primers specific for the nascent (top row) and spliced (middle row) *mCherry* RNA, performed on reverse-transcribed RNA isolated from the indicated MosSCI integration strains. Amplification from a control rDNA spacer transcript, *its-1*, is shown in the bottom row. All amplifications are dependent on reverse transcription (RT) and are therefore not caused by contaminating DNA. Amplicon signals are visible even though the levels for both nascent and spliced *mCherry* are reduced in the mutant constructs.

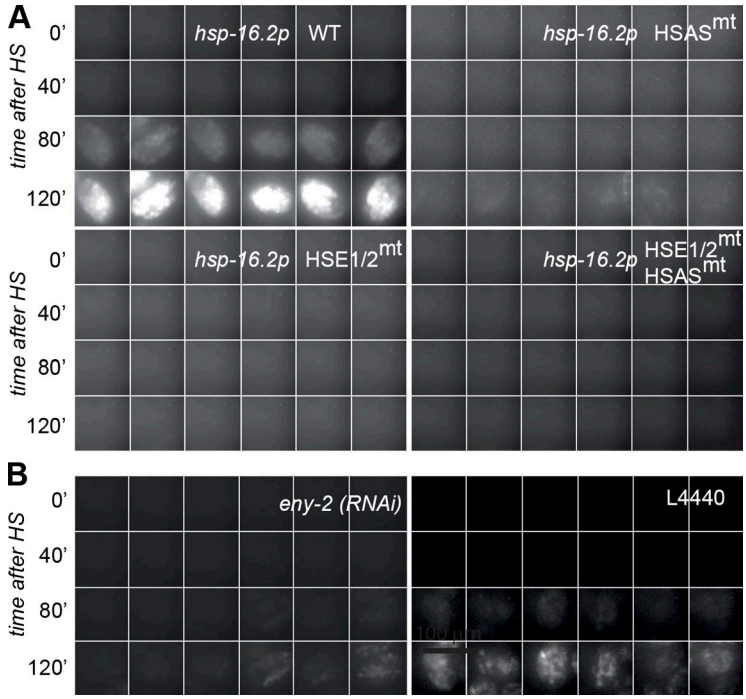

Figure S4. **mCherry protein detection after HS induction.** (A) Red fluorescence signal from mCherry protein in 24 whole embryos from worms carrying the WT or mutated *hsp-16.2* promoter MosSCI insertions driving *mCherry,* as described in Fig. 5 B and scored in Fig. 5 C. The same contrast and brightness was applied to all images. (B) mCherry red fluorescence signal from embryos of the progeny of control RNAi or *eny-2(RNAi)* fed adults as scored in Fig. 7 B. The same contrast and brightness was applied to all images.

Table S1. **Overview of *C. elegans* strains used including genetic details**

Strain name	Genotype	Arrays/transgenes
N2	*WT Bristol isolate*	
GW76	*gwIs4[myo-3::rfp baf-1::gfp-lacI let-858 3′UTR] X*	**Large array**
GW102	*gwIs4 [myo-3::rfp baf-1::gfp-lacI let-858 3′UTR] X; gpIs1[hsp-16.2::gfp]*	**Large arrays**
GW220	*gwIs4 [myo-3::rfp baf-1::gfp-lacI let-858 3′UTR] X; gpIs1[hsp-16.2::gfp] hsf-1(sy441)I*	**Large arrays**
GW391	*gwIs49[hsp-16.2::mCherry 256xLacO 4xLexA; unc-119(+)]; unc-119(ed3) III; gwIs39[baf-1::GFP-LacI::let-858 3′UTR; vit-5::GFP] III*	**Small transgene**/large array
GW421	*gwIs58[hsp-16.2::mCherry 256xLacO 4xLexA; unc-119(+)]; unc-119(ed3) III; gwIs39[baf-1::GFP-LacI::let-858 3′UTR; vit-5::GFP] III*	**Small transgene**/large array
GW432	*gwIs28[myo-3::wmCherry unc-119(+) 256 x LacO 4xLexA; unc-119(+)]; gwIs39[baf-1::GFP-LacI::let-858 3′UTR; vit-5::GFP] III; unc-119(?) III*	**Small transgene**/large array
GW440	*gwSi0[256x lacO; unc-119(+)]; gwIs39[baf-1::GFP-LacI::let-858 3′UTR; vit-5::GFP] III; unc-119(ed3) III*	**MosSCI**/large array
GW615	*gwSi3[hsp-16.2::wmCherry; 256x lacO; unc-119(+)]; gwIs39[baf-1::GFP-LacI::let-858 3′UTR; vit-5::GFP] III; unc-119(ed3) III*	**MosSCI**/large array
GW644	*gwSi5[hsp-16.2 HSE1/2^{mt}::wmCherry; 256x lacO; unc-119(+)]; gwIs39[baf-1::GFP-LacI::let-858 3′UTR; vit-5::GFP] III; unc-119(ed3) III*	**MosSCI**/large array
GW648	*gwSi9[hsp-16.2 HSAS^{mt}HSE1/2^{mt}::wmCherry; 256x lacO; unc-119(+)]; gwIs39[baf-1::GFP-LacI::let-858 3′UTR; vit-5::GFP] III; unc-119(ed3) III*	**MosSCI**/large array
GW649	*gwSi10[hsp-16.2 HSAS^{mt}::wmCherry; 256x lacO; unc-119(+)]; gwIs39[baf-1::GFP-LacI::let-858 3′UTR; vit-5::GFP] III; unc-119(ed3) III*	**MosSCI**/large array
GW597	*gwIs58[hsp-16.2::mCherry 256xLacO 4xLexA; unc-119(+)]; unc-119(ed3) III; gwIs39[baf-1::GFP-LacI::let-858 3′UTR; vit-5::GFP] II; dpy-13(e184) ama-1(m118m251) IV*	**Small transgene**/large array
GW691	*gwIs58[hsp-16.2::mCherry 256xLacO 4xLexA; unc-119(+)]; unc-119(ed3) III; gwIs39[baf-1::GFP-LacI::let-858 3′UTR; vit-5::GFP] III; dpy-13(e184) ama-1(m118m238) IV*	**Small transgene**/large array
GW692	*gwSi13[256x lacO @ ttTi9115; unc-119(+)]V; unc-119(ed3)III; gwIs39[baf-1::GFP-LacI::let-858 3′UTR; vit-5::GFP] III*	**MosSCI**/large array
GW815	*gwSi16[hsp-16.2/41::mCherry 2x]; unc-119(ed3)III; gwIs39 [baf-1::GFP-LacI::let-858 3′UTR; vit-5::GFP]III*	**MosSCI**/large array
GW820	*gwSi13[256x lacO @ ttTi9115; unc-119(+)]V; unc-119(ed3)III; gwIs39[baf-1::GFP-LacI::let-858 3′UTR; vit-5::GFP] III; dpy-13(e184) ama-1(m118m251)IV*	**MosSCI**/large array
PMW54	*gwIs39[baf-1::gfp-lacI let-858 3′UTR; vit-5::gfp] III; gpIs1[hsp-16.2::gfp]*	**Large array**/large array

Arrays indicated in bold contain *lacO* sites and make a visible spot when combined with GFP-LacI.

Table S2. **Overview of primers used**

Amplified Locus	Sequence (5′-3′)	Forward/reverse	Locus	Used for
mCherry; processed	ATTACGATGCTGAGGTGAAGAC	Forward	Transgene	qPCR on cDNA
mCherry; processed	CGATAGTGTAATCCTCGTTGTG	Reverse	Transgene	qPCR on cDNA
hsp-16.2; processed	ATCTTATGAGAGATATGGCTC	Forward	Endogenous	qPCR on cDNA
hsp-16.2; processed	TTGTTAACAATCTCAGAAGACT	Reverse	Endogenous	qPCR on cDNA
mCherry; nascent	AAGGGTGAAGAAGATAACATGG	Forward	Transgene	qPCR on cDNA
mCherry; nascent	GTCCGCCTTTAGTTACCTGA	Reverse	Transgene	qPCR on cDNA
hsp-16.2; nascent	TGAGTCTTCTGAGGTAAATAA	Forward	Endogenous	qPCR on cDNA
hsp-16.2; nascent	CATTGTTAACAATCTGAAAGC	Reverse	Endogenous	qPCR on cDNA
its-1	CCTGGTGGCTATATGCGTCT	Forward	Endogenous	qPCR on cDNA
its-1	CCGTGAAGACTTTTGGCAAT	Reverse	Endogenous	qPCR on cDNA
intergenic locus on *chr V*	CAAAAAGCGTTTTCAGCACA	Forward	Control	qPCR after ChIP
intergenic locus on *chr V*	TCTGAAGTGGGGAGCTTTGT	Reverse	Control	qPCR after ChIP
intergenic locus on *chr II*	AAGACAAACACTGCCAGAAAA	Forward	Control	qPCR after ChIP
intergenic locus on *chr II*	ATCCTTGACGCCAGTGACAT	Reverse	Control	qPCR after ChIP
hsp-16.2	GGGGATCCAGTGAGATGATT	Forward	Ectopic	qPCR after ChIP
hsp-16.2	ATGTGAGTCGCCCTCCTTTT	Reverse	Ectopic	qPCR after ChIP
hsp-16.2	TGGACGGAAATAGTGGTAAAGTG	Forward	Endogenous	qPCR after ChIP
hsp-16.2	CCTTTTGCAACAAGCAGCTC	Reverse	Endogenous	qPCR after ChIP
hsp-16.2	AAGCCAACACGCTTTGTTCT	Forward	Ectopic/endogenous	qPCR after ChIP
hsp-16.2	TCCAGTGAGTTCGTCCAAGA	Reverse	Endogenous	qPCR after ChIP
hsp-16.2	CGACTCTAGAGGATCAAGAGCA	Reverse	Ectopic	qPCR after ChIP
hsp-16.2	ATTCAGCAGATTTCTCTTCGAC	Forward	Endogenous	qPCR after ChIP
hsp-16.2	GTACGCTATCAATCCAAGGAG	Reverse	Endogenous	qPCR after ChIP
hsp-16.2	CACAAAGGGACAGTTCTGAG	Forward	Endogenous	qPCR after ChIP
hsp-16.2	TAAGATCTAGGAACATCCACAG	Reverse	Endogenous	qPCR after ChIP
hsp-16.2	CTCCTGACTCCAAACTTCTC	Forward	Endogenous	qPCR after ChIP
hsp-16.2	AACATTTCTGCCTTCTCCT	Reverse	Endogenous	qPCR after ChIP
hsp-16.2	GAACATGGATACTTGAAACGCT	Forward	Endogenous	qPCR after ChIP
hsp-16.2	GTGATGAGTTTGTCTTCTTTGG	Reverse	Endogenous	qPCR after ChIP
mCherry	GTCACTGTAACAACTCCTCC	Forward	Ectopic	qPCR after ChIP
mCherry	TTAAACATCCGGCAGATATACC	Reverse	Ectopic	qPCR after ChIP
mCherry	GGAGAAAGAGCATGTAGGA	Forward	Ectopic	qPCR after ChIP
mCherry	TCCCACAACGAGGATTACAC	Reverse	Ectopic	qPCR after ChIP
Cbunc-119	CACAACAAAGCCGACTACTC	Forward	Ectopic	qPCR after ChIP
Cbunc-119	GGGAAGGAACAAACTAGACAG	Reverse	Ectopic	qPCR after ChIP
Cbunc-119	ACCAAACCGATATGAAAGCC	Forward	Ectopic	qPCR after ChIP
Cbunc-119	AAGATACCTTGAGTGATTCCC	Reverse	Ectopic	qPCR after ChIP
lmn-1	CAAGAGAACAACAGACTCCAG	Forward	Endogenous	qPCR copy number
lmn-1	TAATAAGACCACCGCATCAG	Reverse	Endogenous	qPCR copy number
unc-119	CCACACCACCTCTAATCTCC	Forward	Endogenous/tg	qPCR copy number
unc-119	TCATTTCTCTGCGTCTTCCT	Reverse	Endogenous/tg	qPCR copy number
hsp-16.2	TGAATCAGAATATGGAGAACGG	Forward	Endogenous/tg	qPCR copy number
hsp-16.2	GACTCACATTCGGTACATGG	Reverse	Endogenous/tg	qPCR copy number
bla	ATCGTTGTCAGAAGTAAGTTGG	Forward	Tg	qPCR copy number
bla	GCCGCATACACTATTCTCAG	Reverse	Tg	qPCR copy number

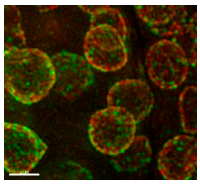

Video 1. **3D reconstruction of WT *C. elegans* embryos stained for nuclear pores and lamina.** WT *C. elegans* embryos were fixed on glass slides and immunostained for nuclear pores (Mab414; green) and nuclear lamina (anti–LMN-1; red). Images were acquired on a super-resolution structured illumination microscope (Elyra system [Carl Zeiss] with an EM-CCD camera [Andor iXon 885]), and the 3D reconstruction was performed with Zen software.